

Charge Amplification of GEM-Based Gas Detectors

Sanghyo HAN^{1,*}, Hyosung CHO^{3,4}, Yongkyun KIM¹, Heedong KANG⁵, Chongun CHUNG¹, Sangmook KANG^{2,4},
Sehwan PARK¹, Jang-Min HAN¹, Yong-Sub CHO¹, Do-Hyung KIM⁵, Young-Jun KIM¹,
Kyoungkeun JEONG¹ and Tae-Hoon LEE¹

¹Korea Atomic Energy Research Institute, Deokjin-dong, Yuseong-gu, Taejeon, Korea

²Department of Medical Engineering, ³Department of Radiation Science, ⁴Research Institute of Medical Engineering, Yonsei University,
Wonju 220-710, Korea

⁵Department of Physics, Kyungpook National University, Taegu 702-701, Korea

The operation of a gas electron multiplier (GEM) detector equipped with a multiwire proportional chamber (MWPC) or a micro strip gas chamber (MSGC) was examined. The additional gain provided by the GEM permitted the operation of the combined detector at substantially reduced voltages, thus increasing its reliability. The GEM + MWPC detector showed a very good gain uniformity of 2% variation throughout the active detector area. The single GEM detector achieved effective gains of above 3000 with pure Ar by the effect of avalanche confinement.

KEY WORDS: *gas electron multiplier, multiwire proportional chamber, micro strip gas chamber, avalanche*

I. Introduction

The recently introduced gas electron multiplier (GEM)¹⁾ is comprised of a thin polymer foil (50 μ m kapton) coated on both sides with metal and perforated with a regular matrix of small holes. The holes are made by etching with a diameter of 60 μ m and a pitch of 100 μ m using conventional photolithographic methods. Under application of a suitable potential difference between the GEM electrodes, the GEM mesh acts as an amplifier for electrons released by radiation in the drift region due to the strong electric field in the holes where external drift field lines are focused. Coupled to main gas avalanche detectors including a standard MWPC or a MSGC, a GEM mesh provides pre-amplification and hence greatly improves the reliability of the device that can be operated at substantially reduced voltages.

The MSGC has been developed and adopted for use in many high-energy physics experiments mainly because of their good rate capability ($\sim 10^6$ Hz/mm²) and excellent position resolution (~ 30 μ m). It has been reported that under a high irradiation rate or exposure to heavily ionizing tracks, occasional transitions from a proportional avalanche to a streamer occur at high operating voltages, followed by a discharge, often resulting in irreversible damage to the fragile strip electrodes and readout electronics. Adding a GEM to an MSGC might reduce the required operating voltage and, consequently, the spark risk; the combined GEM + MSGC detector has been adopted for use in the HERA-B experiments in order to solve the discharge problems in MSGCs^{2,3)}.

This paper describes the operating characteristics

measured with various structures in different gas mixtures. The operation of the GEM in pure Ar was also observed in order to suggest its possible use as a non-aging gas detector.

II. Experimental procedures

Figure 1 shows a schematic diagram of the cross section of the GEM + MWPC and GEM + MSGC detectors used in investigating the operating properties. The drift electrode, an aluminized mylar sheet, is located 3 mm above the GEM and is negatively biased relative to it, thus creating a drift field, E_D , for electrons which are produced by ionization of X-rays in the upper drift region. The gap between the bottom GEM electrode and the MWPC anodes and the gap between the bottom GEM electrode and the MSGC anode, corresponding to the collection region, are 3 mm and 2 mm, respectively. In the single GEM and the GEM + MSGC modes, the collection field (E_C) indicates the electric field in the collection region.

Differences in signal formation in the GEM + MWPC structure can be anticipated, such as direct and pre-amplified signals. The GEM is mounted in the assembly in place of one of the MWPC cathode planes. The MWPC is operated with the anode wires at a positive potential, and the signals are read out through a decoupling capacitor, while the bottom GEM electrode, as well as the MSGC electrodes acting as a second MWPC cathode, is grounded. The anode wires of the MWPC are 15 μ m in diameter and are spaced at a pitch of 3 mm. For a photon released in the lower drift region (between the bottom GEM electrode and MSGC), only the number of primary electrons (N_p) and the gain of the MWPC (G_{mwpc}) contribute to the signal (total charge = $N_p \cdot G_{mwpc}$). On the other hand, the charge released in the

*Corresponding author, Tel. +82-42-868-2716, Fax. +82-42-861-6950 E-Mail; twios96@hananet.net

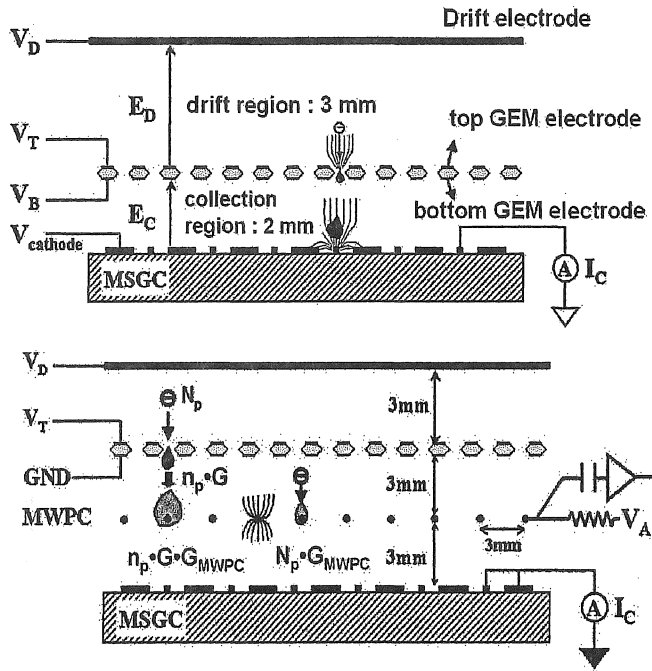


Fig. 1. Schematic view of (top) a GEM + MWPC and (bottom) a GEM + MSGC detection mode. In a single GEM detection mode, MSGC anodes and cathodes are at ground potential.

upper drift region is amplified twice, once in the GEM and once in the MWPC. A fraction of the primary electrons and the electrons multiplied in the GEM channels become captured by the top and the bottom GEM electrodes, so a charge loss factor, T , has been included in the total charge signal, $N_p \cdot G_{mwpc} \cdot G_{GEM} \cdot T$ (G_{GEM} = GEM gain).

In the GEM + MSGC mode, the anodes in the MSGC are at ground potential and can be read out with amplifiers for the pulse-height spectra while the cathodes are connected to a negative high voltage for multiplication of the pre-amplified charge in the GEM. In the single GEM and the GEM + MWPC modes, groups of MSGC anodes and cathodes were connected together and grounded through a picoammeter; the MSGC was not operated. For the MSGC, alternating anodes and cathodes are patterned with a 0.2- μm -thick layer of Cr on a 0.8-mm-thick Corning 7059 glass substrate by using sputtering and lift-off techniques to ensure a uniform edge profile. The widths of the anode and the cathode are 5 μm and 95 μm , respectively, at a pitch of 200 μm . All measurements were realized by exposing the detector to a 5.9-keV ^{55}Fe X-ray source with a typical detected flux corresponding to 580 $\text{mm}^{-2}\text{s}^{-1}$. For the gain estimate, we measured the signal current, I_S , on the anodes of the MWPC or the MSGC, and the count rate R from the X-ray spectrum separately; the gain is given by $I_S/(RNe)$, where e and N denote the electron charge and the known number of electron-ion pairs per conversion (~ 220 for 5.9 keV in Ar/CO₂(70/30)), respectively. In the single GEM mode, the effective gain is defined by $I_C/(RNe)$, taking electron charge losses in the bottom GEM electrode into consideration, where a collection current, I_C , is the electron signal current on the anodes and cathodes of the MSGC.

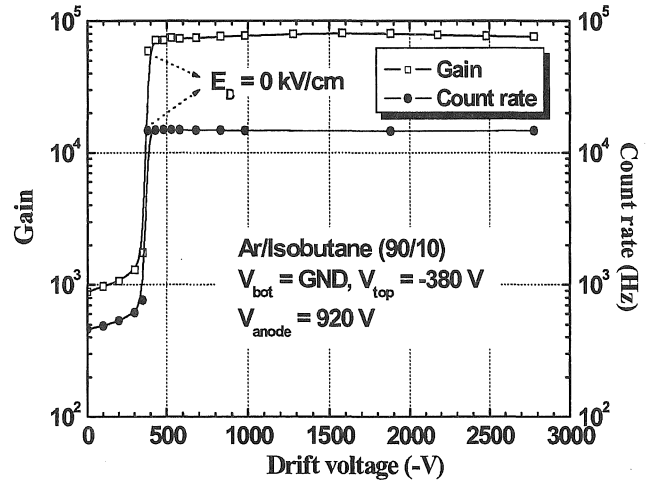


Fig. 2. Count rate and gain as functions of voltage applied to the drift electrode in a GEM + MWPC detector. The GEM voltage and the MWPC anode voltage are set at 380 V and 920 V, respectively.

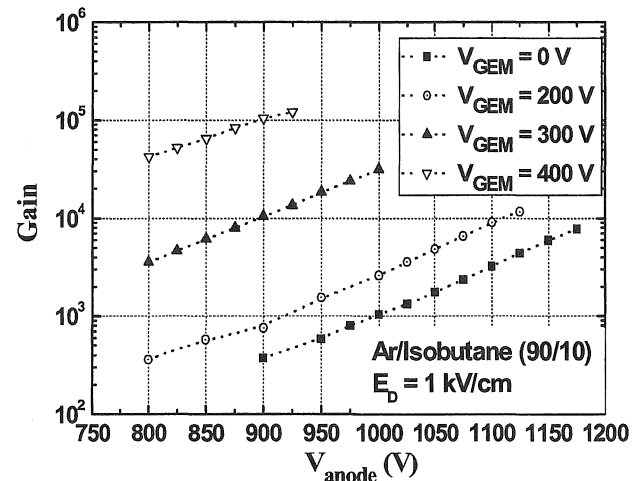


Fig. 3. Gain of a GEM + MWPC detector as a function of the MWPC anode voltage for different GEM voltages in Ar/isobutane (90/10).

III. Experimental results

1. GEM and MWPC operation

In order to determine the appropriate drift field, we examined the gain and count rate of the GEM + MWPC detector as functions of the drift voltage in a gas mixture of Ar/isobutane (90/10) (see Fig. 2). When the drift voltage is below -400 V, the gain and count rate are very small. At around -400 V, both the gain and the count rate increase abruptly and are nearly constant for drift voltages up to -1500 V, which indicates efficient electron collection. At very low drift fields, some electrons do not pass the GEM hole due to increases in diffusion and recombination or to sweeping back to the drift electrode, resulting in signal losses.

The combined gain of the GEM + MWPC detector is shown in Fig. 3 as a function of the anode voltage in the MWPC for different GEM voltages. The curve labeled $V_{GEM}=0$ V in the figure corresponds to a pure MWPC

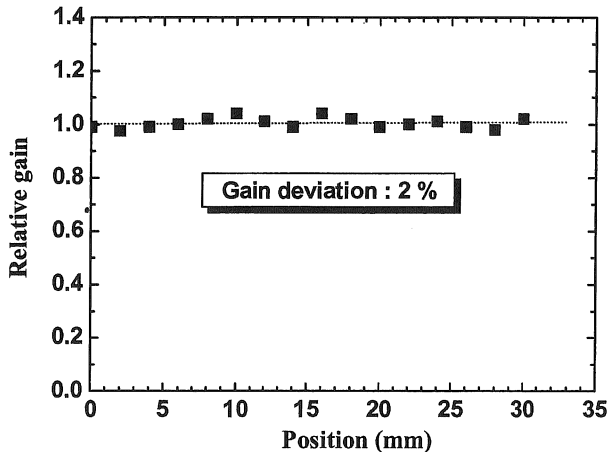


Fig. 4. Gain uniformity in a GEM + MWPC detector.

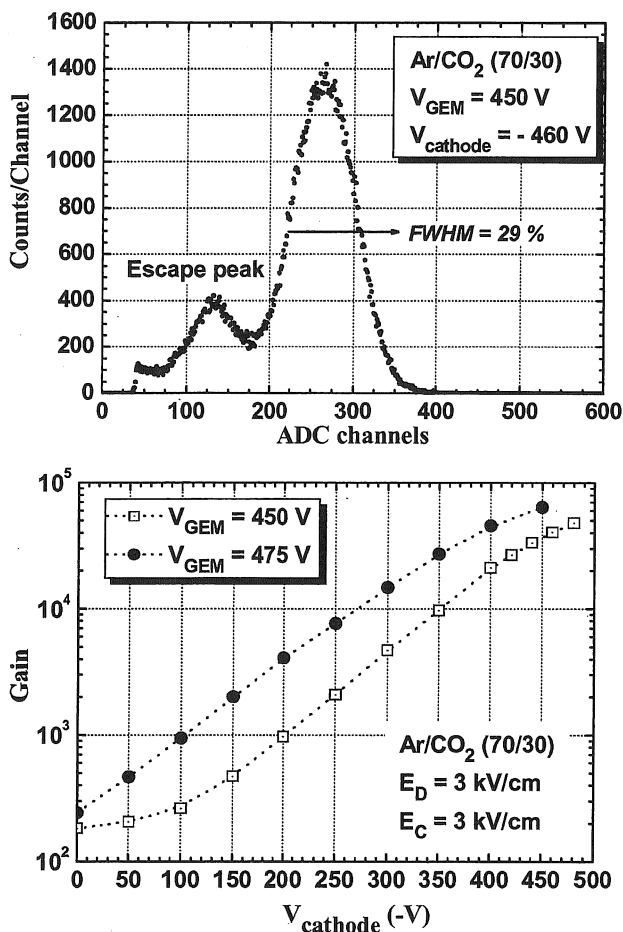


Fig. 5. (top) ^{55}Fe pulse-height spectrum recorded at a gain of 4×10^4 and (bottom) gain in a GEM + MSGC detection mode.

operating mode in which only ionization released in the lower drift region is detected. All other gain curves represent the charge produced in the upper drift region, which is pre-amplified by the GEM before being multiplied by the MWPC. The maximum gain of the GEM + MWPC detector approaches 10^5 at $V_{\text{GEM}} = 400$ V and $V_{\text{Anode}} > 900$ V.

To cover large active areas, it is of high importance that the response of the whole detector surface is homogeneous. The gain uniformity of the GEM + MWPC detector has been

measured by displacing the collimated source with a diameter of 1 mm across the active area. The gain uniformity is very good, with a deviation of 2% (see Fig. 4), as compared with a result of previous studies⁴). Since the gain has a strong dependence on the hole size and the thickness of the insulator, this shows the high precision of the manufacturing which was reached.

2. GEM and MSGC operation

We have observed that the GEM + MSGC detector shows very high overall gains, allowing a much safer operation mode for the MSGC, which can be operated at a lower voltage. Figure 5 shows a typical pulse-height spectrum for the doubly multiplied charge due to the GEM and the MSGC, and the gain of a GEM + MSGC detector as a function of the cathode voltage in the MSGC. The energy resolution at the main peak was calculated to be 29% FWHM for the 5.9 keV ^{55}Fe X-ray source. Gas gains well above 10^4 were observed at a very reduced MSGC operation voltage of around 350 V in a nonflammable gas mixtures of Ar/CO₂ (70/30), thus reducing the discharge problems.

A new mode of operation using a MSGC at zero cathode voltage, the single GEM detector, has been reported^{5,6}). The single GEM detector allows signal detection in the ionization mode on the MSGC; the signal is the result of induction from the movement of the electron cloud produced in the avalanche within the GEM channel.

To understand the operation of the single GEM detector, we simulated an electric field by using MAXWELL⁷) and GARFIELD⁸) field simulators. Figure 6 shows the influence of the drift and the collection fields on charge sharing in a single GEM detector. The higher the ratio E_D/E_{GEM} (E_{GEM} = the average field in the GEM hole and depends on the GEM voltage) and the lower the ratio E_C/E_{GEM} , the larger the fraction of drift field lines terminating on the GEM bottom electrode instead of the collection electrode. In an actual case, a strong drift field directs some electrons to the top GEM electrode, as well as to the bottom GEM electrode, due to diffusion, resulting in signal losses.

Non-aging gas detectors are in considerable demand for the development of gas photomultipliers⁹⁻¹¹) in which the photocathodes are extremely reactive to the impurities created by an avalanche. Monatomic noble gases do not decompose in the avalanche and, thus, do not lead to aging, but the maximum gas gain achievable is rather low in the existing gas avalanche detectors due to their poor quenching properties. It has recently been reported that the GEM can effectively operate in a pure noble gas, such as Ar or Xenon, at fairly high gains of above 1000¹²).

Figure 7 shows the effective gain of a single GEM as a function of the GEM voltage in pure Ar at different collection fields. One can see that the maximum gain attainable is around 3000 at very low GEM operating voltages. This is much higher gain than that reported by the CERN group¹³) using a GEM with 80- μm hole diameter and 140- μm pitch and can be explained by the higher electric field in the multiplication channels due to the smaller GEM

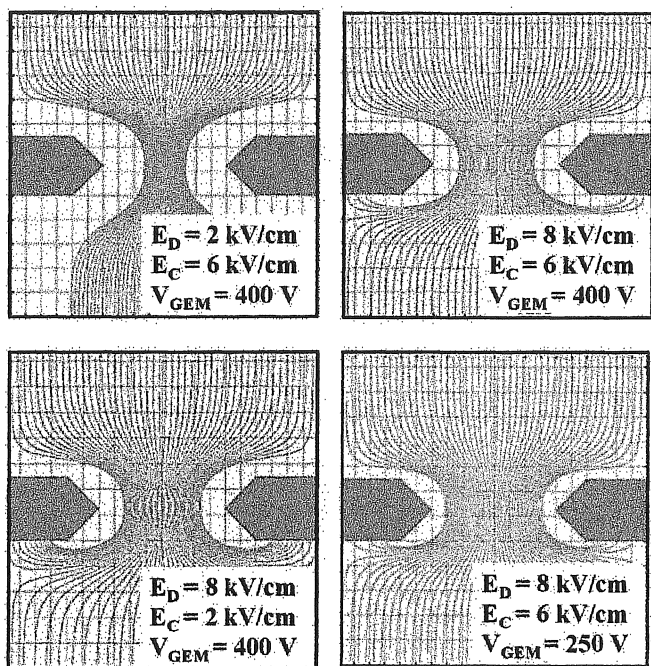


Fig. 6. Drift field line simulation of a single GEM mode for different external field strengths and applied GEM voltages.

holes. In addition, the avalanche confinement in the GEM microholes¹⁴⁾ is another source of high gain; the smaller GEM holes can effectively suppress photon-induced secondary avalanches. As demonstrated in earlier papers^{15,16)}, a field-dependent fraction of the electron charge in the avalanche is collected on the bottom electrode; the fraction is a function of the ratio E_C/E_{GEM} . The higher the ratio E_C/E_{GEM} , the larger the fraction of electron charge detected on the collection electrode. The ratio E_C/E_{GEM} was kept constant during each measurement so as to guarantee the identical electron transfer.

IV. Conclusions

With the added pre-amplification of the GEM, the GEM + MWPC or GEM + MSGC detector showed very high gains of around 10^5 GEM. When coupled to a MSGC, the additional gain provided by the GEM permits a lower MSGC operation voltage, providing a solution to possible discharge problems in MSGCs. No serious gain variation was observed, with a deviation of 2% across the active detector area. In pure Ar, a very high GEM gain of around 3000 was obtained in a single GEM detector, which can be attributed to the smaller GEM holes and the avalanche confinement in the GEM holes.

Acknowledgment

Thanks are due to F. Sauli and R. De Oliveira of CERN who provided the GEMs used in this work.

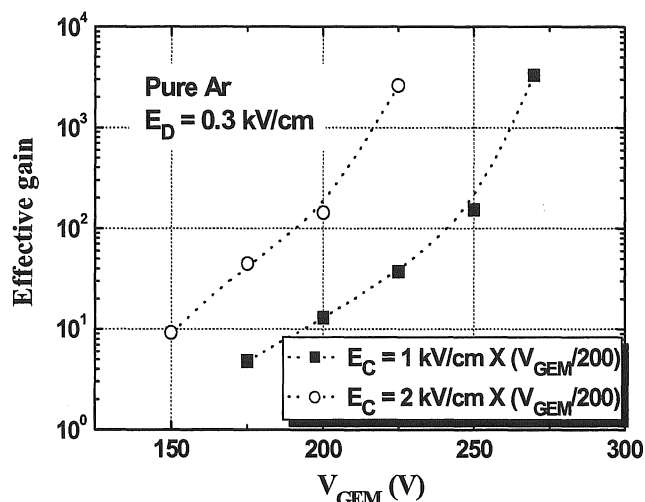


Fig. 7. Effective gain of a single GEM with respect to the GEM voltage measured in pure Ar at two different collection electric fields. For identical electron transfer, the collection field (E_C) was set to be proportional to the GEM voltage (V_{GEM}) during each measurement.

References

- 1) F. Sauli, Nucl. Instr. Meth. A 386, 531 (1997).
- 2) A. Oed, Nucl. Instr. Meth. A 263, 351 (1988).
- 3) B. Schmidt, Nucl. Instr. Meth. A 419, 230 (1998).
- 4) A. Bressan, J-C. Labbé, P. Pagano, L. Ropelewski, and F. Sauli, Nucl. Instr. Meth. A 425, 262 (1999).
- 5) Sanghyo Han, Heedong Kang, Yongkyun Kim, Byungsoo Moon, Chongun. Chung, Hyosung Cho, and Sangmook Kang, Submitted to the proceedings of ISORD-2 (Sendai, Jul., 2003).
- 6) R. Bouclier, W. Dominik, M. Hoch, J-C. Labbé, G. Million, L. Ropelewski, F. Sauli, A. Sharma, and G. Manzin, Nucl. Instr. Meth. A 396, 50 (1997).
- 7) MAXWELL electric field simulator, Ansoft Co., Pittsburg, PA, USA.
- 8) R. Veenhof, Nucl. Instr. Meth. A 419, 726 (1998).
- 9) V. Peskov, E. Silin, Nucl. Instr. Meth. A 367, 347 (1995).
- 10) A. Buzulutskov, E. Shefer, A. Breskin, R. Chechik, M. Prager, Nucl. Instr. Meth. A 400, 173 (1997).
- 11) E. Shefer, A. Breskin, A. Buzulutskov, R. Chechik, M. Prager, Nucl. Instr. Meth. A 419, 612 (1998).
- 12) A. Buzulutskov, L. Shekhtman, A. Breskin, , A. Di Mauro, L. Ropelewski, F. Sauli, and S. Biagi, Nucl. Instr. Meth. A 433, 471 (1999).
- 13) A. Bressan, A. Buzulutskov, L. Ropelewski, F. Sauli, and L. Shekhtman, Nucl. Instr. Meth. A 423, 119 (1999).
- 14) A. Bondar, A. Buzulutskov, F. Sauli, L. Shekhtman, Nucl. Instr. Meth. A 419, 418 (1998).
- 15) Sanghyo Han, Heedong Kang, Yongkyun Kim, Byungsoo Moon, Chongun. Chung, Hyosung Cho, Sangmook Kang, J. Korean Phys. Soc. 40, 820 (2002).
- 16) J. Benlloch, A. Bressan, M. Capeans, M. Gruwé, M. Hoch, J-C. Labbé, A. Placci, L. Ropelewski, and F. Sauli, Nucl. Instr. Meth. A 419, 410 (1998).